

FILE COPY

84148

1 of 2 cys.

Semiannual Technical Summary

Integrated Optical Circuits

30 June 1975

Prepared for the Defense Advanced Research Projects Agency
under Electronic Systems Division Contract F19628-73-C-0002 by

Lincoln Laboratory

MASSACHUSETTS INSTITUTE OF TECHNOLOGY

LEXINGTON, MASSACHUSETTS



Approved for public release; distribution unlimited.

IDA022695

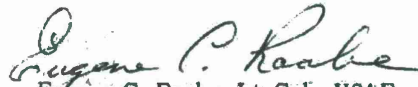
The work reported in this document was performed at Lincoln Laboratory, a center for research operated by Massachusetts Institute of Technology. This work was sponsored by the Defense Advanced Research Projects Agency under Air Force Contract F19628-73-C-0002 (ARPA Order 2074) and is being monitored by Air Force Cambridge Research Laboratories.

This report may be reproduced to satisfy needs of U.S. Government agencies.

The views and conclusions contained in this document are those of the contractor and should not be interpreted as necessarily representing the official policies, either expressed or implied, of the Defense Advanced Research Projects Agency of the United States Government.

This technical report has been reviewed and is approved for publication.

FOR THE COMMANDER



Eugene C. Raabe, Lt. Col., USAF
Chief, ESD Lincoln Laboratory Project Office

Non-Lincoln Recipients

PLEASE DO NOT RETURN

Permission is given to destroy this document
when it is no longer needed.

MASSACHUSETTS INSTITUTE OF TECHNOLOGY
LINCOLN LABORATORY

INTEGRATED OPTICAL CIRCUITS

SEMIANNUAL TECHNICAL SUMMARY REPORT
TO THE
DEFENSE ADVANCED RESEARCH PROJECTS AGENCY

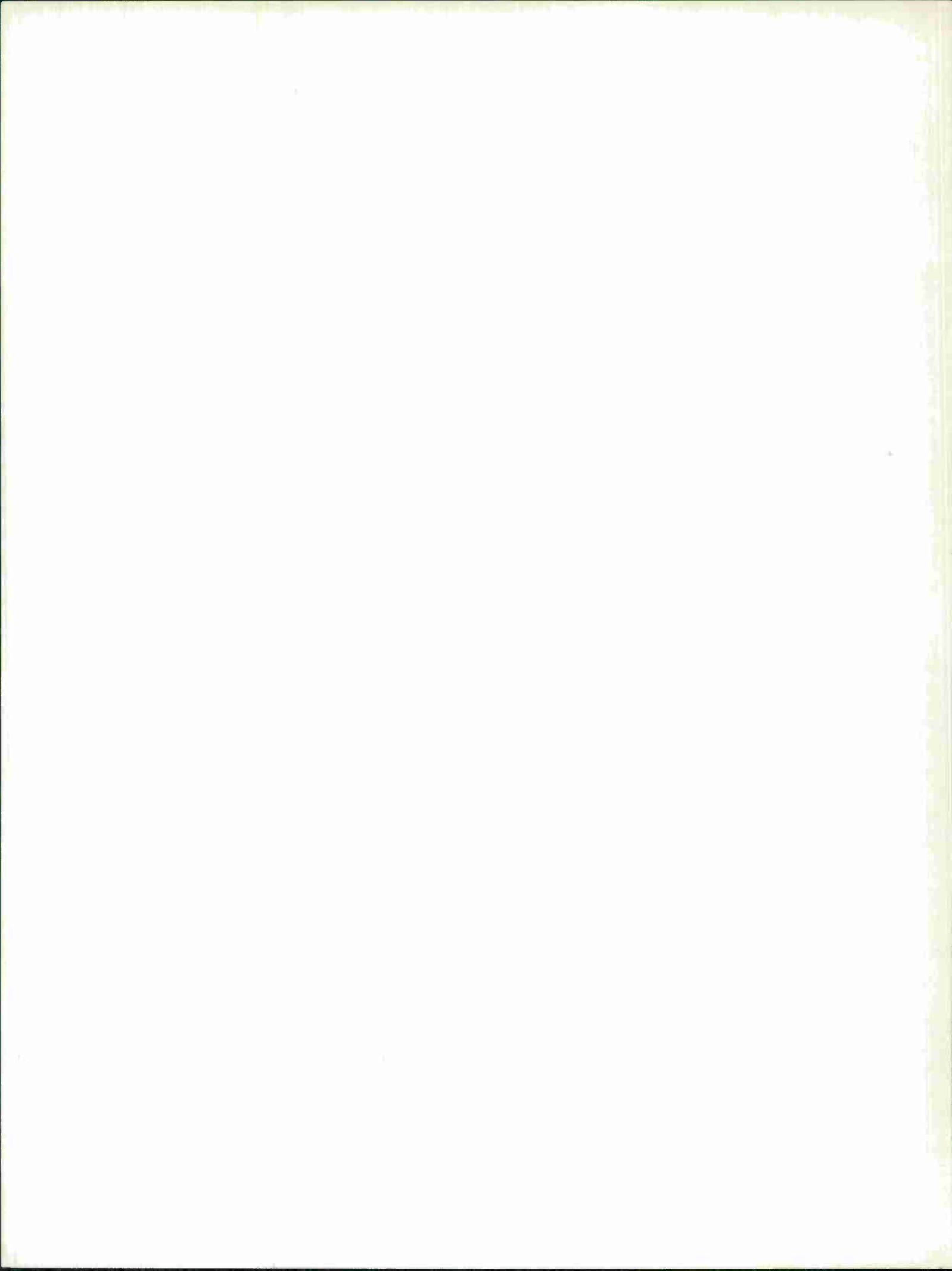
1 JANUARY - 30 JUNE 1975

ISSUED 22 JANUARY 1976

Approved for public release; distribution unlimited.

LEXINGTON

MASSACHUSETTS



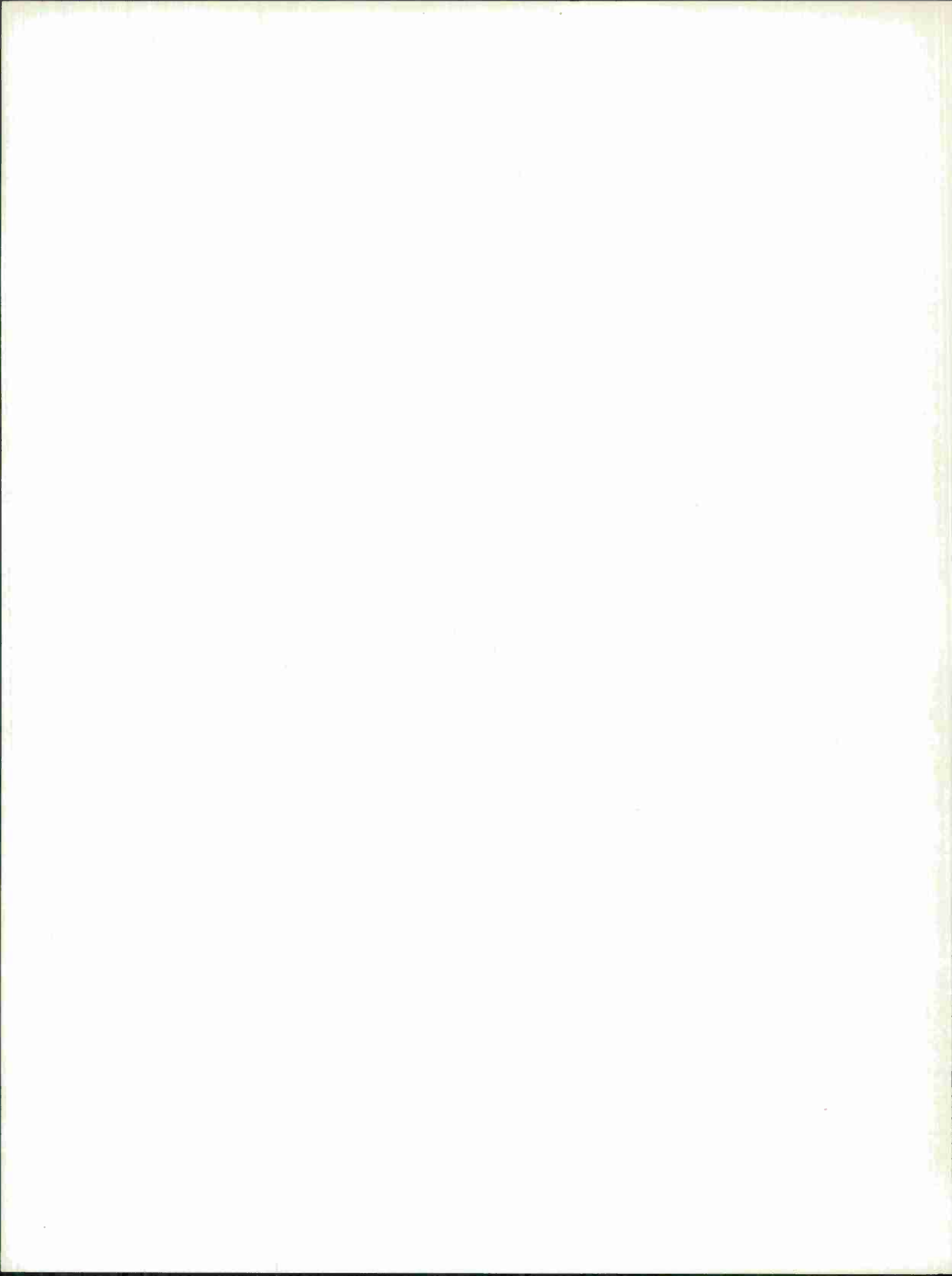
ABSTRACT

Attenuation measurements in epitaxial n-GaAs waveguides of different purity have been made near the absorption edge. These measurements show that losses of $<2 \text{ cm}^{-1}$ can be achieved at energies within 50 meV of the band edge using material with $N_D + N_A \leq 2 \times 10^{15} \text{ cm}^{-3}$, a level of purity which is attainable with current vapor-phase, liquid-phase, and molecular-beam epitaxial growth techniques.

The electroabsorption coefficient of GaAs has been measured in uniform electric fields at wavelengths from 0.91 to 0.93 μm . These measurements were made using Schottky-barrier contacts on low-loss GaAs waveguides, and the experimental results are in good agreement with theoretical calculations of the Franz-Keldysh effect. Electroabsorption detectors with subnanosecond response time and 100-percent internal quantum efficiency have been integrated into these waveguides, and small values of avalanche gain have been obtained without any intentional guardring structure. Integrated electroabsorption modulators with >20 dB depth of modulation have also been fabricated.

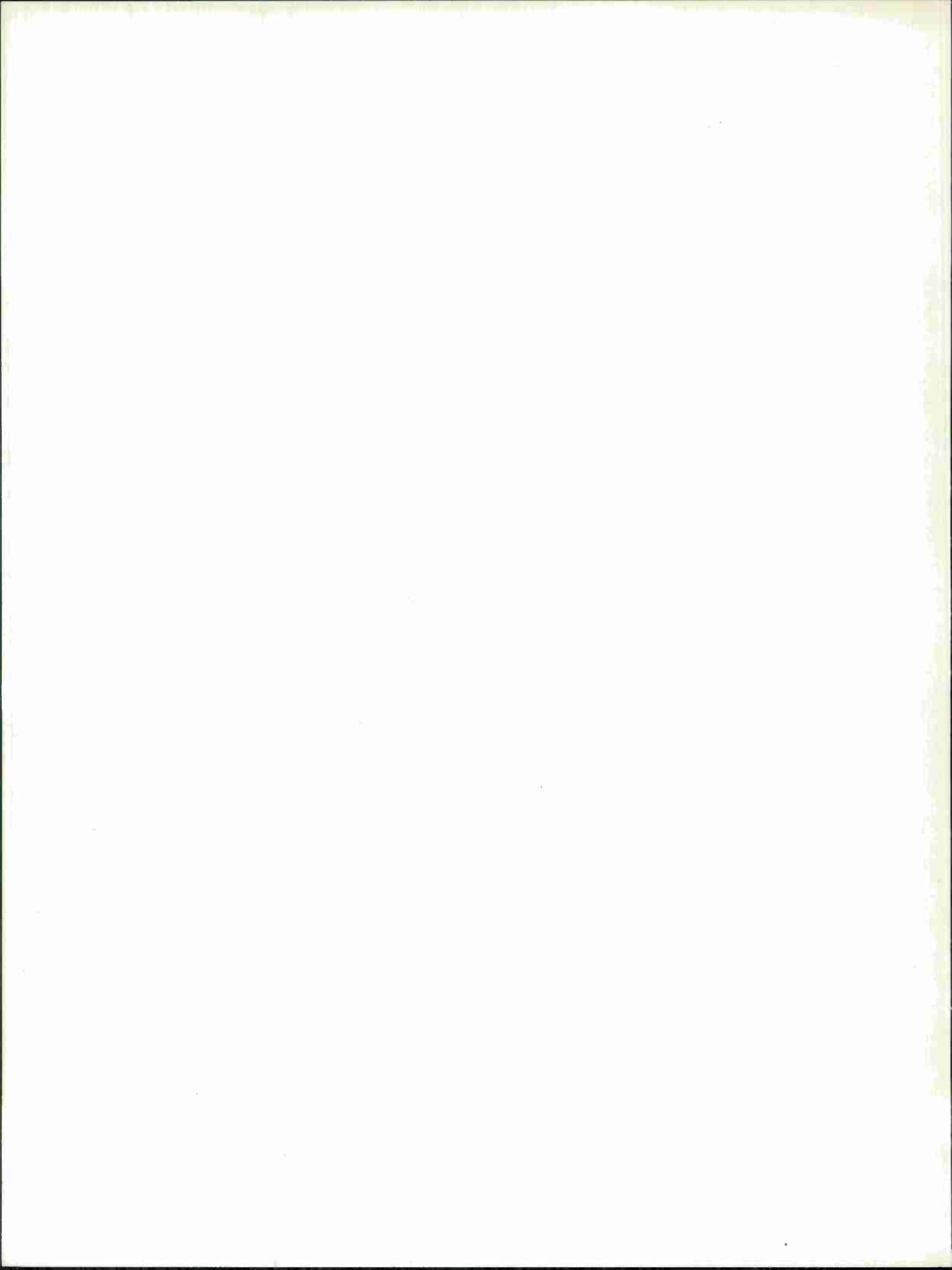
A Schottky-barrier electroabsorption modulator has been combined with a GaAs-AlGaAs laser integrated into a high-purity GaAs waveguide to form a completely integrated IOC source. Over 11 dB of modulation was obtained with a modulator having active length of only 45 μm .

PbSnTe liquid-phase epitaxial layers have been grown on top of $\lambda/2$ gratings fabricated in PbTe to form PbSnTe heterostructure distributed feedback laser structures. Scanning electron micrographs show no etch-back or degradation of the gratings.



CONTENTS

Abstract	iii
I. GaAs-Based Integrated Optical Circuits	1
A. Low-Loss High-Purity GaAs Waveguides	1
B. Electroabsorption Measurements in GaAs and Applications to Waveguide Modulators and Detectors	2
C. Integrated GaAs-AlGaAs Laser and Electroabsorption Modulator	6
II. Lead-Salt Integrated Optical Circuits: Distributed Feedback $\text{Pb}_{1-x}\text{Sn}_x\text{Te}$ Lasers	7
References	9



INTEGRATED OPTICAL CIRCUITS

I. GaAs-BASED INTEGRATED OPTICAL CIRCUITS

A. LOW-LOSS HIGH-PURITY GaAs WAVEGUIDES

Previously reported¹ loss measurements on high-purity GaAs waveguides have been extended to guides with higher impurity concentrations in order to determine the dependence of transmission loss on guide purity. The results indicate that losses remain low ($\alpha < 2 \text{ cm}^{-1}$ for $\lambda > 0.904 \text{ } \mu\text{m}$) for total impurity concentrations up to about $2 \times 10^{15} \text{ cm}^{-3}$.

The measurements were made using tunable grating-controlled GaAs lasers and a Nd:YAG laser, as reported previously.¹ Sample in-sample out measurements at each wavelength were made on two or more different lengths of guide, and the exponential loss coefficient and attenuation were calculated from the results of these measurements. The waveguides measured were all epitaxial layers between 5 and 20 μm thick, and were grown on GaAs substrates ($n = 1 \times 10^{18} \text{ cm}^{-3}$) using an AsCl_3 vapor-phase growth system. Although in theory these guide thicknesses and this substrate doping should permit the propagation of several modes, spatial scans of the emitted intensity from the output cleaved edge of these waveguides indicated that the lowest-order mode was always preferentially excited. Since the losses for the higher-order modes are greater than that for the lowest-order mode, these measurements should be representative of loss coefficients that can be achieved in single-mode waveguides of the same purity, as long as scattering at the epitaxial layer-substrate interface is not significant.

Figure 1 shows the wavelength variation of the attenuation and exponential loss coefficients for three planar GaAs waveguides of different purity. The epitaxial material for the waveguides designated by the circular and triangular data points in this figure was undoped GaAs,

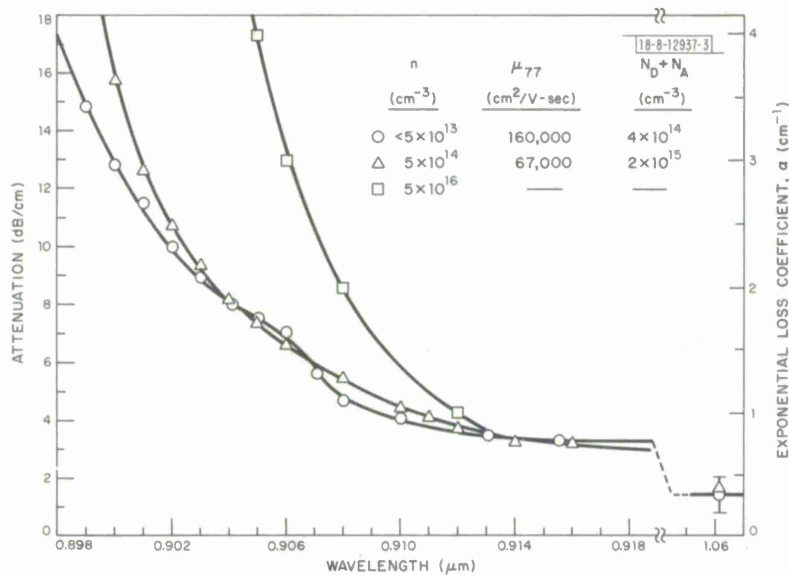


Fig. 1. Attenuation of three different GaAs n^- on n^+ waveguides at wavelengths close to absorption edge.

with carrier concentrations $< 5 \times 10^{13} \text{ cm}^{-3}$ and $5 \times 10^{14} \text{ cm}^{-3}$, respectively, and corresponding 77 K mobilities of 160,000 and 67,000 $\text{cm}^2/\text{V}\text{-sec}$, while that for the waveguide denoted by the square data points was intentionally doped with Sn to give a carrier concentration of $5 \times 10^{16} \text{ cm}^{-3}$. The estimated total ionized impurity concentrations for the three samples were 4×10^{14} , 2×10^{15} , and $\geq 5 \times 10^{16} \text{ cm}^{-3}$, respectively. The loss coefficients shown were calculated from transmission measurements on waveguides of three different lengths (1.4, 0.9, and 0.5 cm) made from the same material. The error bars on the points at 1.06 μm in Fig. 1 are typical of the uncertainty in the measurements throughout the entire wavelength range. For the purest waveguide material (circles), there is a gradual increase in α from 0.3 cm^{-1} at 1.06 μm to 0.7 cm^{-1} at 0.915 μm . For shorter wavelengths the increase is more rapid, reaching 0.95 cm^{-1} at 0.910 μm and 1.5 cm^{-1} at 0.905 μm . The more rapid increase in the loss at the shorter wavelengths is due to the nearness of the absorption edge. The "tail" of the absorption at these wavelengths is probably due to the Franz-Keldysh effect associated with the internal electric fields in the crystal that result from ionized impurities or other crystal defects.^{2,3} The small shoulder at 0.905 μm for this sample must involve some other impurity absorption mechanism. Optical absorption⁴ and photoconductivity⁵ also were observed previously at this wavelength, but the defect responsible has not been identified. The triangular data points in Fig. 1 show the wavelength variation of the absorption coefficient for waveguides with epitaxial layers that have a total ionized impurity content about a factor-of-five greater than the highest purity sample. As shown, there is very little difference in the loss coefficient for these two samples at the longer wavelength (i.e., $\lambda \geq 0.905 \mu\text{m}$), and the increased absorption due to the Franz-Keldysh effect of the electric fields associated with the ionized impurities only becomes significant for wavelengths shorter than about 0.902 μm . It is interesting to note that there is no evidence of the absorption shoulder at 0.905 μm for this sample. For lowest loss waveguides in this wavelength range, it will be important to choose material in which this absorption shoulder is minimized. The square data points in Fig. 1 show the wavelength variation of the loss coefficient for waveguides made from deliberately doped epitaxial material. In this case the absorption in the near-band-edge region is much higher, and waveguides from this material would not be as suitable for use for integrated electroabsorption modulators and detectors in this spectral region.

From the results presented above, it is clear that for GaAs epitaxial layers with total ionized impurity concentrations of less than about $2 \times 10^{15} \text{ cm}^{-3}$, the planar waveguide losses are sufficiently low to permit their use in IOCs at wavelengths that can be achieved with GaAs heterostructure lasers. GaAs material of the required purity can be easily prepared by vapor-phase, liquid-phase, and molecular-beam epitaxial techniques. Furthermore, it has already been shown that these low-loss guides are highly compatible with the integration of heterostructure lasers and electroabsorption detectors and modulators (see p. 3 in Ref. 1, and Sec. B below).

G. E. Stillman
C. M. Wolfe
J. A. Rossi

B. ELECTROABSORPTION MEASUREMENTS IN GaAs AND APPLICATIONS TO WAVEGUIDE MODULATORS AND DETECTORS

In an earlier report⁶ and in recent publications,^{5,7} the electroabsorption effect in GaAs and its application to the fabrication of discrete GaAs EAP photodiodes with response out to about 0.95 μm were described. Utilizing Schottky-barrier contacts on high-purity GaAs waveguides

similar to those described in the previous section, we made quantitative measurements of the electroabsorption effect and fabricated both electroabsorption modulators and detectors fully integrated into the guides. It was possible to measure the electroabsorption effect under the nearly uniform field conditions attainable in these low-loss waveguides, whereas previous measurements⁸⁻¹⁰ had been confined to p-n junctions on heavily doped material where the electric field was highly nonuniform. The integrated electroabsorption detectors had nearly 100-percent internal quantum efficiency and response times which were subnanosecond. The waveguide modulators exhibited >20-dB modulation depth, and the measurements indicate that electroabsorption modulators requiring <0.1-mW/MHz driving power should be attainable with three-dimensional waveguides.

The GaAs waveguides were fabricated by growing high-purity epitaxial layers on (100)-oriented $1 \times 10^{18} \text{ cm}^{-3}$ n-type substrates using the $\text{AsCl}_3\text{-H}_2\text{-Ga}$ vapor-phase technique. The epitaxial layer used for the measurements reported here was high resistivity and had a net electron concentration of $<10^{13} \text{ cm}^{-3}$, as estimated from zero-bias capacitance measurements on Au Schottky barriers. The layer was $10 \text{ }\mu\text{m}$ thick and was fully depleted at zero bias. Electroplated Au Schottky barriers in the form of stripes were oriented perpendicular to the direction of propagation of the radiation in the waveguide and parallel to the cleaved ends of the waveguide into which the radiation was end-fire coupled (see Fig. 2). To permit the measurement of a range of absorption coefficients, stripes of three different widths (0.25, 0.50, and 1 mm) were used. An alloyed Au-Sn ohmic contact was formed on the substrate, and the reverse-bias voltage was applied between any combination of the Schottky-barrier stripes and this ohmic contact. Because of the low carrier concentration in the waveguide layer, the electric field across the guide was nearly uniform, and the average electric field was determined by dividing the applied voltage by the waveguide thickness. For these Schottky-barrier contacts, electric fields as high as $2 \times 10^5 \text{ V/cm}$ could be applied before breakdown occurred around the perimeter of the device.

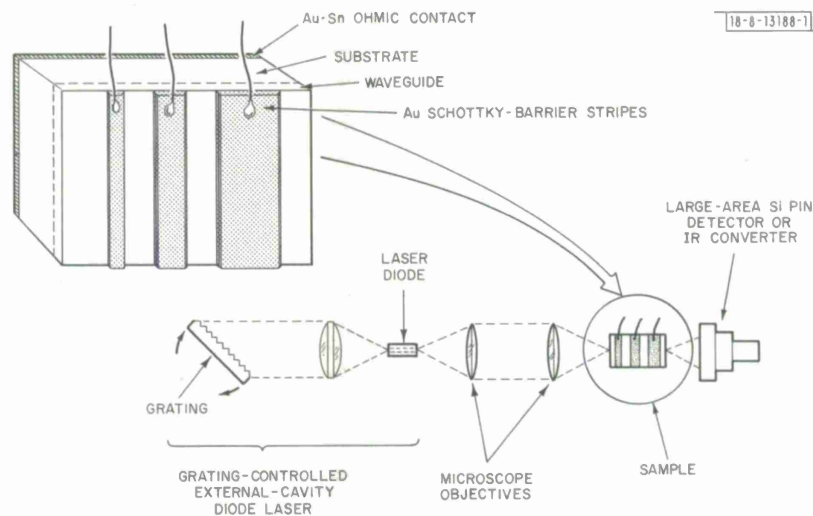


Fig. 2. Experimental arrangement used for measurement of electroabsorption coefficient of GaAs. Inset shows configuration of Schottky-barrier-stripe contacts used to establish uniform electric field in high-purity GaAs waveguide.

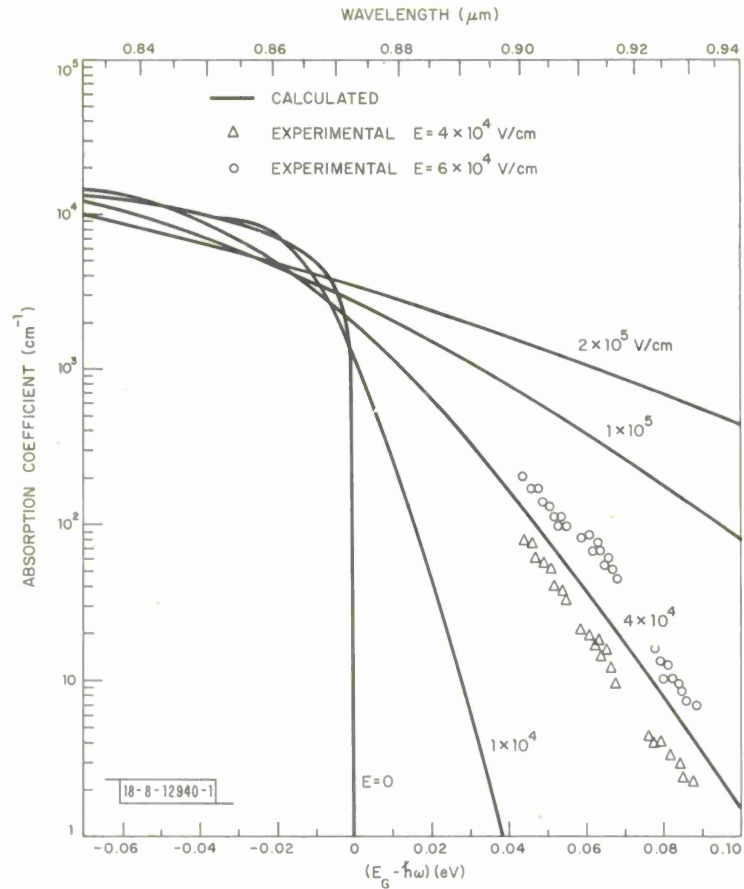


Fig. 3. Calculated and experimental absorption coefficients for GaAs at various electric fields.

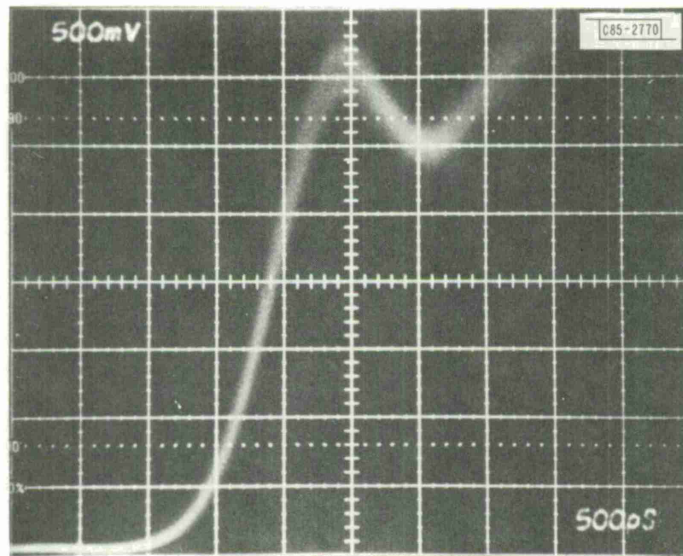


Fig. 4. Leading edge of pulse response of integrated GaAs electroabsorption detector to laser diode radiating at $\lambda = 0.91 \mu\text{m}$.

The electroabsorption measurements were made with the same apparatus previously used to measure the transmission of high-purity GaAs waveguides at wavelengths close to the band edge.¹ The arrangement used is shown schematically in Fig. 2. To obtain quantitative measurements, the waveguide-laser diode combination was first aligned using an infrared microscope. The transmission of the waveguide as a function of the electric field applied to the different Schottky-barrier stripes was then measured by means of a large-area Si PIN photodiode. The magnitude of the electroabsorption was determined from these transmission measurements using the width of the appropriate stripe and neglecting any small changes in reflectivity or coupling efficiency that may be induced by the application of the bias voltage.

For a comparison of the experimental results with theory, the Franz-Keldysh electroabsorption coefficient for GaAs was calculated using the expressions derived by Tharmalingham¹¹ and Callaway¹²:

$$\alpha(\omega, E) = \frac{1.0 \times 10^4}{n} E^{1/3} \sum_j \left(1 + \frac{m}{m_{v_j}}\right) \left(\frac{2\mu_j}{m}\right)^{4/3} \left\{ \left| \left(\frac{dAi(z)}{dz}\right)_{\beta_j} \right|^2 - \beta_j |Ai(\beta_j)|^2 \right\}$$

where $\beta_j = 1.1 \times 10^5 (E_g - \hbar\omega) (2\mu_j/m)^{1/3} E^{-2/3}$, Ai is the Airy function, and the sum is over the light- and heavy-hole valence bands. In this equation, the zero-field interband matrix element has been approximated by using the f-sum rule,¹³ and for the numerical calculations the parameters were: $n = \text{constant} = 3.63$, $m_{v_1}/m = 0.087$, $\mu_1/m = 0.0377$, $m_{v_2}/m = 0.450$, $\mu_2/m = 0.0579$, and $E_g = 1.42$ (Ref. 14). Because of the uncertainty in the matrix elements used here, the calculated absorption was multiplied by a constant factor (0.58) to obtain agreement with experimental zero-field absorption measurements¹⁴ at energies slightly greater than the bandgap energy.

The results of the experimental measurements and theoretical calculations are shown in Fig. 3. The experimental absorption is plotted for electric fields of 4×10^4 and 6×10^4 V/cm. Although fields as high as 1 to 2×10^5 V/cm could be applied to the devices before breakdown occurred at the edge of the Schottky-barrier contacts, the quantitative electroabsorption measurements were restricted to fields no greater than 6×10^4 V/cm because of the possible effects of field nonuniformity. In addition, for attenuation values of 20 dB or more there was a residual transmission similar to that described by Dymant and Kapron¹⁵ which prevented accurate electroabsorption measurements for electric fields $> 6 \times 10^4$ V/cm with the smallest width Schottky-barrier stripe used. The experimental variation of the electroabsorption with wavelength is in good agreement with the calculated curves, and in view of the accuracy of the matrix elements used in the theoretical calculation, the agreement between the calculated and experimental absorption values is satisfactory.

The integrated electroabsorption detectors were simply 1.25-mm-diameter Schottky barriers electroplated on top of the waveguides described above. The leading edge of the pulse response of one of the detectors is shown in Fig. 4. The excitation source was a pulsed (50-nsec) GaAs laser radiating at $0.91 \mu\text{m}$, and the output of the electroabsorption detector was direct-coupled into the 50-ohm termination of the oscilloscope. The observed rise time is approximately 1 nsec, which is approximately the rise time of the oscilloscope. For three-dimensional waveguides,¹⁶ the area of the detector can be much smaller and it should be possible to attain response speeds approaching the transit time limit. By measuring the radiation into and out of the waveguide and the variation of the photocurrent with bias voltage, it was determined that the

internal quantum efficiency of the device was approximately 100 percent for bias voltages ≥ 20 V. At the higher bias voltages, avalanche gain was observed, but it was limited to a value of about 4 for a bias voltage of 200 V ($E = 2 \times 10^5$ V/cm). To obtain larger values of avalanche gain, it will be necessary to provide some form of guarding to prevent edge breakdown.

The Schottky-barrier stripe on the n^- waveguide used for the electroabsorption measurement is, in itself, an integrated modulator structure, and the measured attenuation in excess of 20 dB translates directly into a depth of modulation of the same amount. The use of the electroabsorption effect for the modulation and detection of light has been known for some time.¹⁷ Application of the effect to devices for modulation¹⁸ has been of limited usefulness because of the large insertion loss usually encountered at wavelengths close to the absorption edge. However, these electroabsorption devices have negligible loss over that of the low-loss waveguides themselves. A calculation using these measured electroabsorption parameters indicates that, for a three-dimensional single-mode waveguide of 5- μm thickness and 10- μm width, the power requirements of an electroabsorption modulator with 99-percent modulation efficiency at 0.91 μm can be < 0.1 mW/MHz, and will probably be limited by the stray capacitance rather than by the actual device capacitance.

G. E. Stillman
C. M. Wolfe
J. A. Rossi

C. INTEGRATED GaAs-AlGaAs LASER AND ELECTROABSORPTION MODULATOR

The Schottky-barrier electroabsorption modulator described in the previous section has been combined with an integrated double-heterostructure GaAs-AlGaAs laser (see p. 3 in Ref. 1) to produce a source suitable for incorporation into an IOC. The structure, shown schematically in Fig. 5, was fabricated by electroplating an Au Schottky-barrier contact directly on the top surface of the high-purity GaAs waveguide portion of an integrated etched-mesa laser. The modulator contact was 45 μm long (in the direction of light propagation) by about 100 μm wide.

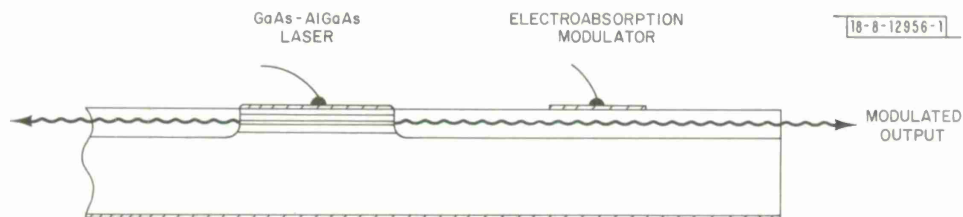


Fig. 5. Artist's representation of integrated GaAs-AlGaAs laser-waveguide-electroabsorption modulator structure.

For the Schottky barriers on these waveguides ($N_D - N_A \sim 1 \times 10^{15} \text{ cm}^{-3}$), breakdown occurred for a bias of about 100 V. The observed modulation was a maximum just below breakdown, reaching a value of 11 dB. At this bias, the 12- μm -thick waveguide was just depleted and the high-field region extended over only a fraction of the guide thickness. Based on the results reported in the previous section, it is expected that with a higher-purity waveguide and a somewhat longer modulator, a depth of modulation in excess of 20 dB could be easily obtained.

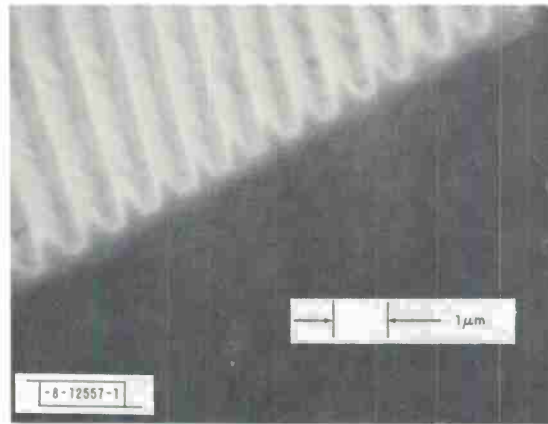
C. E. Hurwitz
J. A. Rossi
G. E. Stillman

II. LEAD-SALT INTEGRATED OPTICAL CIRCUITS: DISTRIBUTED FEEDBACK $\text{Pb}_{1-x}\text{Sn}_x\text{Te}$ LASERS

Considerable progress has been made toward the attainment of distributed feedback laser emission in $\text{Pb}_{1-x}\text{Sn}_x\text{Te}$ diodes operating in the vicinity of $10\ \mu\text{m}$. An initial group of diode laser structures with internal gratings has been fabricated, but DFB operation has not yet been achieved.

The fabrication of the devices is similar to that used successfully for making GaAs distributed feedback lasers.¹⁹ The procedure begins by ion-beam etching a grating with a period of $\lambda/2n_e$ on an electrochemically polished surface of thallium-doped PbTe. Here, λ is the free-space emission wavelength of the laser, and n_e is the effective index of the laser waveguide. Next, a $2\text{-}\mu\text{m}$ layer of $\text{Pb}_{1-x}\text{Sn}_x\text{Te}$ followed by a $1\text{-}\mu\text{m}$ layer of PbTe is grown by liquid-phase epitaxy over the entire grating. Stripe-etched mesas are then formed using photolithographic techniques with the stripes perpendicular to the grating grooves. The end faces of the diode laser cavities are cleaved, thus forming a combined Fabry-Perot and distributed feedback laser structure. This configuration was chosen to facilitate the optical alignment of the laser using the assured Fabry-Perot mode of operation. By temperature-tuning the diode emission to the wavelength for Bragg reflection from the grating, the single-mode operation of the distributed feedback laser should be observed.

Fig. 6. Scanning electron micrograph of grating ion beam etched into PbTe substrate using photoresist mask.



A scanning electron micrograph of one of the gratings obtained on the PbTe is shown in Fig. 6. The surface corrugations shown here were produced by ion-milling or sputter-etching through a photoresist mask produced by the interference pattern of two Ar ion laser beams, as described by others²⁰ for the fabrication of gratings on GaAs. Unfortunately, little work has been reported on the determination of the refractive index of $\text{Pb}_{1-x}\text{Sn}_x\text{Te}$, the value of which is necessary to determine the correct grating period. Even if dispersion effects near the band edges are neglected, reported values of n vary from 6.5 to 6.9 for $\text{Pb}_{0.78}\text{Sn}_{0.12}\text{Te}$ at 77 K (Refs. 21 and 22). At 6 K, the index is slightly higher.²² Using index values of 6.9 for $\text{Pb}_{0.78}\text{Sn}_{0.12}\text{Te}$, 6.25 for PbTe, a free space wavelength of $10.6\ \mu\text{m}$, and a guide thickness of $2\ \mu\text{m}$, an effective index of 6.70 was calculated for the highest-gain TE_0 mode. This corresponds to a first-order grating period of $7908\ \text{\AA}$, and is the value chosen for three initial experiments.

The best liquid-phase epitaxial growth in $\text{Pb}_{1-x}\text{Sn}_x\text{Te}$ is obtained by growing rapidly from a supersaturated melt.²³ These are ideal conditions for growing on a grating because there is no meltback and the short growth time of 3 to 5 min. is insufficient for significant interdiffusion to occur. Consequently, the mechanical and optical integrity of the grating is accurately preserved beneath the epitaxial layer. Although a scanning electron micrograph of sufficient quality to reproduce here was not obtained, it was clear from the observed images on the SEM screen that the gratings were not degraded after the epitaxial growth.

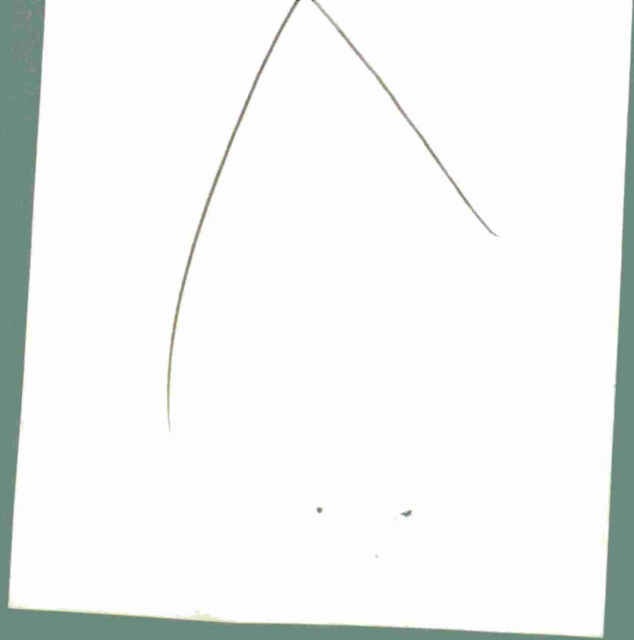
To date, only one group of diode lasers fabricated with the grating structure has been tested. Although the Fabry-Perot operation was observed, the single distributed feedback mode was not seen. The most likely reason for the absence of DFB laser action is an incorrect grating period. Since the uncertainty of the refractive index of $\text{Pb}_{1-x}\text{Sn}_x\text{Te}$ is so large, it will be necessary to fabricate several lasers having grating periods spanning the range of uncertainty in order to ascertain the correct value.

A. R. Calawa
S. H. Groves

REFERENCES

1. Integrated Optical Circuits Semiannual Technical Summary, Lincoln Laboratory, M.I.T. (31 December 1974), p. 1, DDC AD-A014254/7.
2. D. Redfield, *Phys. Rev.* **130**, 916 (1963).
3. G. E. Stillman, D. M. Larsen, and C. M. Wolfe, *Phys. Rev. Lett.* **27**, 989 (1971), DDC AD-737156.
4. D. Bois, *J. de Physique* **35**, C3-241 (1974).
5. G. E. Stillman, C. M. Wolfe, J. A. Rossi, and J. L. Ryan, in Gallium Arsenide and Related Compounds (Institute of Physics, London, 1975), p. 210.
6. Integrated Optical Circuits Semiannual Technical Summary, Lincoln Laboratory, M.I.T. (30 June 1974), p. 1, DDC AD-A006813/0.
7. G. E. Stillman, C. M. Wolfe, J. A. Rossi, and J. P. Donnelly, *Appl. Phys. Lett.* **25**, 671 (1974), DDC AD-A006705/8.
8. T. S. Moss, *J. Appl. Phys.* **32**, 2136 (1961).
9. C. M. Penchina, A. Frova, and P. Handler, *Bull. Am. Phys. Soc.* **9**, 714 (1964).
10. F. K. Reinhart, *Appl. Phys. Lett.* **22**, 372 (1973).
11. K. Tharmalingham, *Phys. Rev.* **130**, 2204 (1963).
12. J. Callaway, *Phys. Rev.* **134**, A998 (1964).
13. J. Bardeen, F. J. Blatt, and L. H. Hall, in Photoconductivity Conference, R. G. Breckenridge, B. R. Russell, and E. E. Hahn, Eds. (Wiley, New York, 1956), p. 146.
14. D. D. Sell and H. C. Casey, *J. Appl. Phys.* **45**, 800 (1974).
15. J. C. Dymant and F. P. Kapron, Proceedings of 5th Biennial Conference on Active Semiconductor Devices for Microwave and Integrated Optics, Cornell, 1975 (to be published).
16. F. A. Blum, D. W. Shaw, and W. C. Holton, *Appl. Phys. Lett.* **25**, 116 (1974).
17. R. C. Eden and P. D. Coleman, *Proc. IEEE* **51**, 1776 (1963).
18. J. C. Dymant, F. P. Kapron, and A. J. SpringThorpe, in Gallium Arsenide and Related Compounds (Institute of Physics, London, 1975), p. 200.
19. D. R. Scifres, R. D. Burnham, and W. Streifer, *Appl. Phys. Lett.* **25**, 203 (1974); D. B. Anderson, R. R. August, and J. E. Coker, *Appl. Opt.* **13**, 2742 (1974); H. M. Stoll and D. H. Seib, *Appl. Opt.* **13**, 1981 (1974); and M. Nakamura, K. Aiki, Jun-ichi Umeda, A. Yariv, H. W. Yen, and T. Morikawa, *Appl. Phys. Lett.* **25**, 487 (1974).
20. H. L. Garvin, E. Garmire, S. Somekh, H. Stoll, and A. Yariv, *Appl. Opt.* **12**, 455 (1973).
21. G. Dionne and J. C. Woolley, *Phys. Rev.* **6B**, 3898 (1972).
22. H. A. Lyden, *Phys. Rev.* **135**, A514 (1964).
23. S. H. Groves, Electronic Materials Conference, Boston, 1974 [abstract: *J. Electron. Mater.* **3**, 863 (1974)].

REPORT DOCUMENTATION PAGE		READ INSTRUCTIONS BEFORE COMPLETING FORM
1. REPORT NUMBER ESD-TR-75-328	2. GOVT ACCESSION NO.	3. RECIPIENT'S CATALOG NUMBER
4. TITLE (and Subtitle) Integrated Optical Circuits		5. TYPE OF REPORT & PERIOD COVERED Semiannual Technical Summary 1 January - 30 June 1975
		6. PERFORMING ORG. REPORT NUMBER
7. AUTHOR(s) Hurwitz, Charles E.		8. CONTRACT OR GRANT NUMBER(s) F19628-73-C-0002
9. PERFORMING ORGANIZATION NAME AND ADDRESS Lincoln Laboratory, M. I. T. P.O. Box 73 Lexington, MA 02173		10. PROGRAM ELEMENT, PROJECT, TASK AREA & WORK UNIT NUMBERS ARPA Order 2074 Program Element No. 61101E
11. CONTROLLING OFFICE NAME AND ADDRESS Defense Advanced Research Projects Agency 1400 Wilson Boulevard Arlington, VA 22209		12. REPORT DATE 30 June 1975
		13. NUMBER OF PAGES 16
14. MONITORING AGENCY NAME & ADDRESS (if different from Controlling Office) Air Force Cambridge Research Laboratories Hanscom AFB Bedford, MA 01731		15. SECURITY CLASS. (of this report) Unclassified
		15a. DECLASSIFICATION DOWNGRADING SCHEDULE
16. DISTRIBUTION STATEMENT (of this Report) Approved for public release; distribution unlimited.		
17. DISTRIBUTION STATEMENT (of the abstract entered in Block 20, if different from Report)		
18. SUPPLEMENTARY NOTES None		
19. KEY WORDS (Continue on reverse side if necessary and identify by block number)		
Integrated Optical Circuits	electroabsorption modulators	$Pb_{1-x}Sn_xTe$
electroabsorption effect	electroabsorption detectors	distributed feedback
GaAs	lasers	gratings
epitaxial growth	Schottky barrier	optical waveguide
20. ABSTRACT (Continue on reverse side if necessary and identify by block number)		
<p>Attenuation measurements in epitaxial n-GaAs waveguides of different purity show that losses of $<2 \text{ cm}^{-1}$ can be achieved at energies within 50 meV of the band edge using material with $N_D + N_A \leq 2 \times 10^{15} \text{ cm}^{-3}$.</p> <p>The electroabsorption coefficient of low-loss GaAs waveguides has been measured in uniform electric fields at wavelengths from 0.91 to 0.93 μm. Electroabsorption detectors and modulators have been integrated into these waveguides. A Schottky-barrier electroabsorption modulator has been combined with a GaAs-AlGaAs laser integrated into a high-purity GaAs waveguide to form a completely integrated IOC source.</p> <p>PbSnTe liquid-phase epitaxial layers have been grown on top of $\lambda/2$ gratings fabricated in PbTe to form PbSnTe heterostructure distributed feedback laser structures.</p>		



Printed by
United States Air Force
Hanscom Air Force Base
Bedford, Massachusetts